



OPEN Potential subtype-specific alterations in gut microbiota and branched-chain amino acid metabolism in hydrogen- and methane-predominant small intestinal bacterial overgrowth

Ziteng Wang^{1,2}, Wentao Tan³, Pengfei Zhang⁴, Huanhuan Xiong⁵, Licun Zhu⁶, Jianfang Cui¹, Li Li¹, Chunmei Guo¹, Lingling He², Jiali Huang¹, Hongshan Wei²✉ & Hong Liu¹✉

We aimed to investigate the clinical, microbiome, and metabolomic characteristics of hydrogen (H₂)- and methane (CH₄)-predominant small intestinal bacterial overgrowth (SIBO) subtypes. We retrospectively enrolled adults who underwent standardized lactulose hydrogen–methane breath testing between February 2021 and July 2025. Participants were categorized as Normal, H₂-SIBO, CH₄-SIBO, or mixed H₂/CH₄-SIBO. Clinical characteristics were compared using Kruskal–Wallis tests and chi-square tests. Multivariable logistic regression was used to identify factors independently associated with each SIBO subtype. Expiratory gas profiles (AUC, peak, and mean values) were quantified, and correlations with age and body mass index (BMI) were assessed using Spearman analysis. In a subset of participants, stool samples underwent 16S rRNA gene sequencing and untargeted metabolomic profiling, followed by integrative analyses of microbiota composition, diversity, and metabolic signatures across SIBO subtypes. Among 503 participants, higher serum albumin levels were independently associated with H₂-SIBO, whereas higher fasting glucose was independently associated with CH₄-SIBO. Breath-test profiling indicated that methane parameters, rather than hydrogen, better differentiated SIBO subtypes, and total (H₂ + CH₄) gas output was modestly correlated with age but not BMI. In the exploratory multi-omics subset, fecal microbiota composition and metabolomic signatures differed by subtype; LEfSe identified *Bacteroidaceae* as a CH₄-SIBO signature and *Alcaligenaceae/ Acidaminococcaceae* as H₂-SIBO signatures. Differential metabolites were enriched in pathways related to branched-chain amino acid biosynthesis, lipid metabolism, and mineral absorption. H₂- and CH₄-predominant SIBO subtypes exhibit distinct clinical correlates and stool microbiome–metabolome profiles. Methane exhalation appears more informative for differentiating subtypes, and age is modestly associated with total expiratory gas volumes. These findings support potential subtype-specific host–microbe metabolic interactions, although the multi-omics results should be interpreted as exploratory.

Keywords Small intestinal bacterial overgrowth, Hydrogen–methane breath test, Gut microbiota, Fecal metabolomics, Branched-chain amino acids

The human gut harbors a complex microbial ecosystem, collectively termed the intestinal microbiota, which includes bacteria, viruses, fungi, archaea, and other microorganisms. These microbes maintain a symbiotic

¹Gastroenterology Department, Beijing Shijitan Hospital, Capital Medical University, Beijing, China. ²Gastroenterology Department, Beijing Ditan Hospital, Capital Medical University, Beijing, China. ³Liver Research Center, Beijing Friendship Hospital, Capital Medical University, Beijing, China. ⁴Emergency Department, Beijing Tiantan Hospital, Capital Medical University, Beijing, China. ⁵Rheumatology and Immunology Department, Zhumadian Central Hospital, Henan, China. ⁶Gastroenterology Department, Shougang Hospital, Peking University, Beijing, China. ✉email: drwei@ccmu.edu.cn; liuhong1118@126.com

relationship with the host and play essential roles in immune regulation, metabolism, and nervous system function¹. Often referred to as the “second genome” of the human body, the intestinal microbiota is critical for maintaining host homeostasis. Its composition varies markedly across anatomical regions: the small intestine contains relatively few microbes, whereas the large intestine exhibits the highest density and diversity of microbial colonization². Microbial load in the small intestine generally ranges from 10^4 – 10^5 CFU/mL in the proximal regions to 10^7 – 10^8 CFU/mL in the distal regions³.

Under normal physiological conditions, the host maintains the small intestinal microbiota within a homeostatic range through several defense mechanisms, including gastric acid bacteriostasis, gastrointestinal myoelectric complex-mediated bacterial clearance, the ileocecal valve barrier, immunomodulatory effects of secretory immunoglobulin A, and the bacteriostatic activity of pancreatic enzymes. Disruption of these mechanisms can lead to microbial imbalance, resulting in small intestinal bacterial overgrowth (SIBO), which is characterized by both increased bacterial abundance and compositional changes, often accompanied by clinical symptoms^{4–6}. SIBO and intestinal methanogenic overgrowth represent major forms of such microbial imbalance, frequently arising from abnormal bacterial migration from the upper gastrointestinal tract or colon into the small intestine^{7,8}.

Pathologically, SIBO involves abnormal colonization by both aerobic and anaerobic bacteria, predominantly gram-negative species such as *Klebsiella pneumoniae*, *Escherichia coli*, and *Clostridium spp.* *Methanogenic archaea*, particularly *Methanobrevibacter smithii*, also contribute significantly to disease pathogenesis. Based on the predominant gas produced during microbial fermentation, SIBO can be classified into hydrogen-dominated (H_2 -SIBO), methane-dominated (CH_4 -SIBO), and hydrogen-methane-dominated (H_2/CH_4 -SIBO) subtypes. H_2 is mainly produced by *Enterobacteriaceae* through carbohydrate fermentation, and H_2 -SIBO patients often present with diarrhea, bloating, and gastrointestinal discomfort. Excess hydrogen can accelerate intestinal peristalsis, disrupt nutrient absorption, and increase the risk of long-term deficiencies in vitamin B12, fat-soluble vitamins, and minerals^{9,10}. In contrast, CH_4 -SIBO is caused by *Methanogenic archaea*, which consume H_2 and CO_2 to produce CH_4 . Elevated methane levels reduce intestinal motility, leading to constipation, abdominal distension, bloating, and reflux. Because hydrogen is converted into methane, standard breath tests may underestimate hydrogen levels, necessitating combined hydrogen-methane testing for accurate diagnosis^{11,12}. H_2/CH_4 -SIBO patients overproduce both gases, often experiencing a combination of diarrhea, constipation, abdominal pain, bloating, reflux, nausea, and chronic fatigue^{13,14}. These observations highlight the need for individualized diagnostic and therapeutic strategies.

Despite growing interest, research on SIBO has largely focused on its general characteristics and disease associations, with limited attention to subtype-specific microbial and metabolic alterations. There is insufficient understanding of species-level distribution, microbial interactions, and their functional impact on host physiology. To address these gaps, we employed a multidimensional approach to systematically analyze SIBO subtypes and their associated gut microbiota, integrating clinical parameters, microbial composition, metabolomic profiles, and functional readouts. Hydrogen and methane breath tests were conducted to quantify expiratory gas volumes, providing functional insights into microbial activity. Univariate and multivariate logistic regression analyses were performed to identify clinical and biochemical factors independently associated with H_2 - and CH_4 -SIBO. Microbial composition was characterized using 16S rRNA sequencing, revealing subtype-specific signatures. Correlation association networks highlighted potential interactions among microbial taxa that may facilitate subtype-specific metabolic activities.

Materials and methods

Research subjects

Between February 2021 and July 2025, we retrospectively screened individuals who had undergone lactulose hydrogen-methane breath tests at Beijing Shijitan Hospital. A total of 503 patients completed the tests. Based on test results, participants were categorized into four groups: SIBO-negative, H_2 -SIBO positive, CH_4 -SIBO positive or H_2/CH_4 -SIBO positive. A subset additionally provided stool samples for exploratory microbiome and metabolomic analyses.

Inclusion criteria

Retrospective study inclusion criteria:

- (1) Age \geq 18 years.
- (2) Completion of the hydrogen-methane breath test.
- (3) Availability of questionnaire data and sufficiently complete clinical records.

Exclusion criteria

Patients were excluded from the study based on the following criteria:

- (1) Gastrointestinal or abdominal surgery: A history of gastrointestinal surgery, abdominal surgery, or any surgery affecting the gastrointestinal system (e.g., gastric bypass, colectomy).
- (2) Renal or infectious diseases: A history of renal insufficiency or other infectious diseases that could impact gastrointestinal function.
- (3) Comorbidity: including but not limited to diseases that may affect gastrointestinal function, such as Crohn's disease, ulcerative colitis, cirrhosis of the liver, hypothyroidism, intestinal obstruction, etc.
- (4) Recent medication use: Use of antibiotics (e.g., amoxicillin, clarithromycin) or drugs that may affect gastrointestinal function (e.g., domperidone) within the past month.

- (5) Recent gastrointestinal issues: A history of enema treatment or acute enteritis in the past week, or malabsorption, or other gastrointestinal diseases.
- (6) Pregnancy and lactation: lactating women or pregnant.
- (7) Intolerance: A known history of lactulose intolerance.
- (8) Study protocol non-compliance: Participants who do not conform to the study protocol, fail to provide informed consent, have not complete personal information that may impact the results, or are unable to fully cooperate with the study procedures.

Data collection and research methods

Collection of basic data

A total of 503 participants completed the breath test and were included in the clinical analysis; 365 had positive hydrogen and/or methane results. Demographic information, including age, sex, height, weight, and body mass index (BMI), was collected. BMI was calculated as weight (kg)/height² (m²). Smoking and alcohol consumption were recorded together with relevant medical histories, including chronic conditions (e.g., hypertension and diabetes) and any history of abdominal surgery or digestive disorders.

After an overnight fast of 6–12 h, venous blood samples were collected in the morning for laboratory testing. Measurements included hematologic indices, liver function markers, metabolic markers, and electrolytes. All assays were performed in the hospital clinical laboratory using routine automated methods. This protocol enabled integrated analysis of clinical characteristics and laboratory markers within the study cohort.

Hydrogen-methane breath test

Patient preparation

Participants were required to follow a standardized preparation protocol before undergoing the lactulose hydrogen-methane breath test (Quintron Corporation, United States) to ensure accurate and reliable results. The protocol consisted of the following steps:

- (1) Fasting requirement: Participants were instructed to fast for a period of 6 to 12 h before the test to eliminate any potential interference with the results.
- (2) Dietary restrictions: Participants were advised to avoid foods that are slow to digest, high in fiber, or known to produce excess hydrogen, for example, pasta, beans, and cereals. Additionally, overeating was discouraged to ensure that digestive processes would not affect the outcomes.
- (3) Medication restrictions: Participants were instructed to refrain from using sedatives or sleep aids on the day preceding the test to prevent any interference with the testing process.
- (4) Smoking prohibition: Refrain from smoking for at least one hour prior to the test to prevent any potential impact on the results.
- (5) Oral hygiene: Prior to the test, participants were required to thoroughly brush their teeth, rinse their mouths, and maintain proper oral hygiene to avoid any contaminants that could influence the test outcome.

Breath test procedure

Participants began the breath test procedure by taking several deep, steady breaths to ensure a relaxed state. Then let them take a deep breath and slowly exhale into the air bag. The first breath air, serving as the baseline measurement. Following the baseline measurement, participants were orally administered 10 mL of lactulose solution (Abbott, Netherlands), and the timing for the test commenced immediately. To ensure accurate results, participants provided subsequent breath samples at 30-min intervals, resulting in a total of six samples. Each exhalation was required to completely fill the designated collection bag to ensure adequate sample volume. To minimize bacterial contamination and interference with test results, participants were instructed to rinse their mouths thoroughly after consuming the lactulose solution.

SIBO diagnostic criteria

Based on the 2020 American Gastroenterological Association clinical practice update, positive breath-test criteria were defined as follows¹⁵:

- (1) H₂ level ≥ 20 ppm from baseline within 90 min after oral lactulose administration.
- (2) CH₄ level ≥ 10 ppm at any time point.

Patient classification based on breath test results

- (1) Normal group: Individuals who exhibited no abnormal elevation in either H₂ or methane CH₄ throughout the test period.
- (2) H₂-SIBO positive group: Individuals demonstrating an increase in H₂ of ≥ 20 ppm above baseline within 90 min following oral lactulose ingestion.
- (3) CH₄-SIBO positive group: Individuals with a CH₄ concentration ≥ 10 ppm at any time point during the breath test.
- (4) H₂/CH₄-SIBO positive group: Individuals who met both criteria for H₂-positive and CH₄-positive SIBO, defined as an H₂ rise ≥ 20 ppm within 90 min and a CH₄ level ≥ 10 ppm at any point during the test.

Fecal sample collection and 16S rRNA sequencing

A total of 30 patients were selected using a 1:2 ratio of SIBO-negative to SIBO-positive individuals through propensity score matching. After excluding one case due to quality control issues, the final sample included

29 participants (10 SIBO-negative and 19 SIBO-positive). Fecal samples were collected using a standardized fecal collection kit (fecal tube 76×20mm; Sarstedt Ag & Co. KG, Germany). The samples were stored at -80°C within 24 h to preserve their integrity. Informed consent was obtained from all participants, and ethical approval was granted by the Ethics Committee of Beijing Shijitan Hospital, affiliated with Capital Medical University (approval no. sjtky11-1x-2022[063]).

To reduce potential confounding arising from overlapping microbial activity, we limited the stool microbiome analyses to SIBO-positive patients with a single dominant expiratory gas. Specifically, only participants who were exclusively H₂-positive or exclusively CH₄-positive were included, while those exhibiting simultaneous positivity for both gases were excluded. This approach was intended to allow a clearer attribution of observed microbial and metabolic signatures to a specific SIBO subtype. We acknowledge that this criterion reduced the number of available samples and may limit the generalizability of the findings; however, it was necessary to minimize interference between hydrogen- and methane-producing microbial communities and to enhance the interpretability of subtype-specific associations.

DNA extraction and 16S rRNA gene amplification

Microbial DNA was extracted using the TianSeq Stool DNA Extraction Kit (TIANGEN, China) according to the manufacturer's instructions. DNA quality was assessed by 1% agarose gel electrophoresis and quantified using a NanoDrop™ 2000 spectrophotometer (Thermo Scientific, USA).

PCR amplification targeted the V3–V4 region of the 16S rRNA gene using the primers 341F (5'-CCTACGGGNGGCWGCAG-3') and 806R (5'-GGACTACHVGGGTWTCTAAT-3'). The PCR protocol consisted of initial denaturation at 95°C for 3 min, followed by 30 cycles of denaturation at 95°C for 30 s, annealing at 55°C for 30 s, and extension at 72°C for 45 s. Each sample underwent three independent PCR amplifications to ensure reproducibility. Sequencing libraries were prepared using the TianSeq Fast DNA Library Prep Kit (Illumina, TIANGEN Biotech), and library quality was assessed using a Qubit™ 2.0 Fluorometer and Agilent Bioanalyzer 2100 system. Sequencing was performed on an Illumina platform using a 2×250 bp paired-end protocol^{16,17,18}.

Microbiome data analysis

Raw sequencing data were processed using the QIIME2 pipeline with the DADA2 plugin. Primer sequences and low-quality regions were trimmed, and reads were denoised to remove sequencing errors and correct amplicon misreads. Exact amplicon sequence variants (ASVs) were inferred, and chimeric sequences were identified and removed using the built-in consensus-based method in DADA2. Representative ASV sequences were taxonomically assigned using the SILVA 138 reference database with a naïve Bayes classifier.

Microbial community profiling included α -diversity metrics (Shannon index, Chao1 richness) and β -diversity based on Bray–Curtis dissimilarity. Differential abundance analyses were performed to identify taxa associated with SIBO subtypes. To reduce confounding from overlapping gas-production profiles, microbiome analyses were restricted to participants exhibiting a single dominant gas phenotype (H₂-only or CH₄-only), excluding mixed H₂/CH₄ producers.

Metabolomics analysis

Human fecal samples (100.0 mg±1.0 mg) were accurately weighed and extracted using pre-cooled methanol:acetonitrile:water (2:2:1, v/v) containing 1 µg/mL deuteriosuccinic acid-D4 as internal standard. Samples underwent vortexing, homogenization with a liquid nitrogen-precooled tissue grinder, and ultrasonic lysis, repeated three times to ensure complete metabolite extraction. Protein precipitates were stored at -40°C for 1 h, followed by centrifugation at 13,800×g for 15 min at 4°C. Supernatants were filtered (0.22 µm) and transferred to LC–MS vials.

Chromatographic separation was performed on a Thermo Vanquish UHPLC system coupled with a Waters ACQUITY UPLC BEH Amide column (2.1×50 mm, 1.7 µm) at 40°C. Mobile phases were: (A) 25 mmol/L ammonium acetate (pH 9.75), (B) acetonitrile, with gradient elution from 95% B to 40% B over 10 min. Flow rate was 0.3 mL/min; injection volume 2 µL; autosampler temperature 4°C. Mass spectrometry was performed on a Thermo Orbitrap Exploris 120 with HESI ion source, full scan range m/z 70–1050, resolution 60,000. Data-dependent acquisition was used for MS/MS fragmentation (HCD 20/30/40 eV, resolution 15,000), and mass accuracy was maintained <2 ppm.

Raw data were converted to mzXML format via ProteoWizard, followed by peak extraction, alignment, and integration using XCMS (v3.16.1; SNR=3; alignment bandwidth=5; minimum fraction=0.5). Metabolite identification was based on BiotreeDB (v3.0) using accurate mass (<5 ppm), retention time, and MS/MS fragment similarity (>80%). Data were normalized using PQN and scaled with UV scaling.

Bioinformatics and statistical analysis

Basic information statistical analysis

Statistical analyses were performed using SPSS version 23.0 (IBM Corp., Armonk, NY, USA). The Kolmogorov–Smirnov test was used to assess normality of continuous variables. Normally distributed variables are presented as mean ± standard deviation and were compared using one-way analysis of variance; non-normally distributed variables are presented as median (interquartile range) and were compared using Kruskal–Wallis tests. Categorical variables are presented as counts and percentages and were analyzed using chi-square tests or Fisher's exact tests, as appropriate. For breath-test profiles, AUC values were calculated and expiratory gas volumes were log-transformed for visualization. Associations of age and BMI with gas volumes were tested using Spearman correlation; linear regression lines and R² values were displayed in scatter plots for descriptive visualization only. Separate logistic regression models were fitted for H₂-SIBO, CH₄-SIBO, and mixed H₂/CH₄-SIBO using

the Normal group as the reference. Candidate variables entered into multivariable models included albumin, glucose, type 2 diabetes, hypertension, smoking, and alcohol consumption. Adjusted odds ratios (aORs) with 95% confidence intervals (CIs) are reported. All tests were two-sided, and $p < 0.05$ was considered statistically significant.

Microbiota analysis

The analysis was conducted using 16S rRNA gene sequencing data processed within the QIIME2 platform (v2020.6). Raw reads were denoised using the DADA2 plugin to remove sequencing noise, trim primers and low-quality bases, infer exact ASVs, and eliminate chimeric sequences. Taxonomic assignment of representative ASVs was performed using a naïve Bayes classifier trained on the SILVA 138 reference database. Downstream ecological analyses were conducted in R (v3.6.2). i) Alpha diversity was evaluated using Observed ASVs, Chao1 richness, Shannon diversity, and Simpson dominance indices. ii) Beta diversity was assessed using Bray–Curtis dissimilarity, followed by principal coordinate analysis (PCoA), principal component analysis (PCA), and orthogonal partial least-squares discriminant analysis (OPLS-DA) to visualize differences among groups. Group-level variation was tested using PERMANOVA. iii) Differential abundance analysis was performed using linear discriminant analysis effect size (LEfSe) with an LDA score threshold of 2.0. Significant taxa were identified using the Kruskal–Wallis rank-sum test, and corresponding effect sizes were calculated. All analyses were performed using the Lianchuan Biotechnology Cloud Platform (Hangzhou Lianchuan Biotechnology Co., Ltd., ICP No. 150250535-4).

For metabolite analysis, PCA, PCoA, and OPLS-DA were conducted using the SIMCA-P (v14.1) software. The criteria for identifying differential metabolites included: i) a variable importance in projection value greater than 1.0; ii) a Student's t-test p-value less than 0.05; and iii) a fold change of at least 2.0. Metabolite annotation was performed using the Kyoto Encyclopedia of Genes and Genomes (KEGG, Release 101.0) databases^{19,20}. Enrichment analysis of metabolic pathways was conducted using the hypergeometric test, with a significance threshold of $p < 0.05$. To evaluate the correlations between bacteria and metabolites, Spearman's rank correlation coefficient was used. Data visualization was performed via the Metware Cloud platform (<https://cloud.metware.cn/>), generating volcano plots and integrated heatmaps.

Results

Retrospective study results

Clinical demographics and correlation analysis of SIBO

The clinical cohort included 503 participants: 138 in the Normal group, 23 in the H₂-SIBO group, 249 in the CH₄-SIBO group, and 93 in the mixed H₂/CH₄-SIBO group (Table 1). Age, sex distribution, BMI, smoking, alcohol use, and the recorded prevalences of type 2 diabetes and hypertension did not differ significantly across groups.

Albumin and fasting glucose differed significantly among the groups. Albumin was highest in the H₂-SIBO group, whereas fasting glucose was highest in the CH₄-SIBO group.

Determinants of H₂- and CH₄-predominant SIBO: findings from univariate and multivariate logistic analyses

To examine host metabolic and lifestyle factors associated with different SIBO phenotypes, we conducted univariable and multivariable logistic regression analyses for H₂-SIBO, CH₄-SIBO, and mixed H₂/CH₄-SIBO (Table 2). In the univariable analysis, higher albumin levels were significantly associated with increased odds of H₂-SIBO, whereas glucose, type 2 diabetes, hypertension, smoking, and alcohol consumption showed no significant associations (Table 2). Albumin remained positively associated with H₂-SIBO, indicating that higher albumin levels modestly increased the likelihood of this subtype. After multivariable adjustment, smoking emerged as an independent factor, demonstrating a potential protective effect against H₂-SIBO. For CH₄-SIBO, higher glucose levels were significantly associated with the methane-producing subtype in both univariable and multivariable analyses. No other variables demonstrated significant associations with CH₄-SIBO. For the mixed H₂/CH₄ subtype, neither univariable nor multivariable analyses identified statistically significant predictors, suggesting that the examined biochemical and lifestyle factors may exert limited or non-specific influence on this mixed pattern.

Analysis of correlation between expiratory volume and SIBO subgroup in hydrogen methane breath test

As shown in Table 3, significant differences were observed in methane-related parameters among SIBO subtypes, while hydrogen-related emissions remained comparable. No significant differences were found in hydrogen AUC (0–90 min, 90–150 min, and total), peak, or mean values across the H₂-SIBO, CH₄-SIBO, and H₂/CH₄-SIBO groups. In contrast, methane parameters differed significantly between groups. Baseline, peak, mean, final CH₄ values, and total CH₄ AUC were all significantly higher in the CH₄-SIBO and H₂/CH₄-SIBO groups compared with H₂-SIBO. Notably, the H₂/CH₄-SIBO group exhibited the highest CH₄ levels and AUC. Additionally, the combined (H₂ + CH₄) total AUC differed significantly among groups ($p = 0.031$), supporting a more prominent role of methane-related output in differentiating subtypes. These findings suggest methane, rather than hydrogen, better differentiates SIBO subtypes and may play a more prominent role in disease pathophysiology.

Correlation analysis of expiratory volume of hydrogen and methane with age and BMI

Figure 1 shows the relationships of hydrogen and methane expiratory volumes with age and BMI. Figure 1a,b show weak, non-significant correlations between hydrogen expiratory volume and both age ($p = 0.3266$, $R^2 = 0.0033$) and BMI ($p = 0.8180$). Similarly, Fig. 1c,d reveal weak associations between methane expiratory volume and age ($p = 0.3771$, $R^2 = 0.0027$) and BMI ($p = 0.5727$), indicating no clear relationships. In contrast, Fig. 1e,f demonstrate a significant positive correlation between the total expiratory volume of hydrogen and

Variable	Subcategory	Normal (n = 138)	H ₂ -SIBO (n = 23)	CH ₄ -SIBO (n = 249)	H ₂ /CH ₄ -SIBO (n = 93)	p-value
Demographics	Age, years	57.00 (41.00–66.00)	56.50 (42.00–60.50)	59.00 (47.75–66.00)	54.50 (40.00–65.25)	0.145
	BMI, kg/m ²	24.49 (21.50–26.89)	25.11 (22.75–25.74)	23.83 (21.69–26.31)	24.22 (22.10–27.14)	0.451
Sex	Male	64 (46.4%)	9 (39.1%)	124 (49.8%)	48 (51.6%)	0.936
	Female	74 (53.6%)	14 (60.9%)	125 (50.2%)	45 (48.4%)	
Lifestyle factors	Smoking	14 (10.1%)	4 (17.4%)	22 (8.8%)	9 (9.7%)	0.255
	Alcohol consumption	16 (11.6%)	1 (4.3%)	27 (10.8%)	9 (9.7%)	0.834
Hematology	Lymphocytes (× 10 ⁹ /L)	1.77 [1.44, 2.26]	1.98 [1.49, 2.28]	1.90 [1.51, 2.27]	1.94 [1.52, 2.22]	0.562
	Monocytes (× 10 ⁹ /L)	0.34 [0.26, 0.40]	0.31 [0.25, 0.44]	0.34 [0.27, 0.43]	0.34 [0.27, 0.42]	0.554
	Neutrophils (× 10 ⁹ /L)	3.37 [2.76, 4.06]	3.72 [2.92, 4.09]	3.29 [2.70, 3.97]	3.41 [2.68, 4.10]	0.554
Inflammation markers	PCT (ng/mL)	0 [0, 0]	0.11 [0.11, 0.11]	0 [0, 0]	0.30 [0.30, 0.30]	0.317
	CRP (mg/L)	0.108 [0.00, 0.286]	0.11 [0.00, 0.43]	0.11 [0.00, 0.10]	0.30 [0.00, 0.30]	0.991
Liver & renal function	WBC (× 10 ⁹ /L)	6.95 [4.77, 9.95]	6.20 [4.30, 7.06]	6.40 [4.44, 10.50]	5.96 [4.19, 12.70]	0.694
	Hemoglobin (g/L)	139 [128, 150]	143 [130, 152]	139 [129, 149]	137 [127, 149]	0.927
	Albumin (g/L)	42.2 [39.3, 44.2]	43.9 [41.5, 46.4]	41.8 [39.3, 43.9]	42.8 [40.2, 44.8]	0.028
	ALT (U/L)	18 [16, 22]	17 [14, 21]	19 [14, 26]	17 [14, 23]	0.707
	AST (U/L)	19 [14, 25]	17 [14, 21.5]	19 [15.5, 23]	18 [15, 23]	0.646
	TBIL (μmol/L)	14.5 [11.15, 17.9]	16.5 [10.5, 21.2]	14.5 [11.85, 18.13]	14.5 [10.9, 18.2]	0.625
	ALP (U/L)	42.2 [39.3, 55]	46.4 [41.5, 56]	41.8 [39.3, 57]	44.8 [40.2, 58]	0.533
	GGT (U/L)	29 [14, 67]	34 [14, 68]	21 [16, 34]	27 [15, 81]	0.059
	Urea (mmol/L)	4.96 [4.28, 5.75]	4.87 [4.24, 6.17]	5.24 [4.44, 6.06]	5.15 [4.19, 5.88]	0.259
	Creatinine (μmol/L)	67 [60, 78]	58 [56, 73]	66 [57, 77]	67.5 [54.8, 78.3]	0.631
Lipids & glucose	TC (mmol/L)	4.47 [3.79, 5.10]	4.14 [4.14, 5.56]	4.56 [3.89, 6.05]	4.55 [3.67, 5.57]	0.572
	Glucose (mmol/L)	5.29 [4.83, 5.69]	5.01 [4.56, 5.46]	5.35 [4.99, 6.05]	5.13 [4.79, 5.57]	0.004
Comorbidities	Type 2 Diabetes	9 (6.5%)	2 (8.7%)	32 (12.9%)	10 (10.8%)	0.487
	Hypertension	24 (17.4%)	4 (17.4%)	53 (21.3%)	23 (24.7%)	0.391

Table 1. Basic characteristics between different subgroups of SIBO. Bold indicates statistically significant difference. *ALT* alanine aminotransferase, *AST* aspartate aminotransferase, *ALP* alkaline phosphatase, *GGT* γ -glutamyltransferase, *CRP* C-reactive protein, *PCT* procalcitonin, *WBC* white blood cell count, *TBIL* total bilirubin, *TC* total cholesterol.

Variable	SIBO type	Univariable OR (95% CI)	p-value	Multivariable OR (95% CI)	p-value
Albumin (g/L)	H ₂	1.155 (1.056–1.264)	0.002	1.115 (1.061–1.173)	0.003
	CH ₄	0.997 (0.946–1.051)	0.915	1.043 (0.951–1.143)	0.375
	H ₂ /CH ₄	1.049 (0.981–1.122)	0.164	1.105 (0.995–1.227)	0.063
Glucose (mmol/L)	H ₂	0.968 (0.566–1.654)	0.904	0.471 (0.148–1.501)	0.203
	CH ₄	1.218 (1.010–1.470)	0.039	1.185 (1.013–1.330)	0.043
	H ₂ /CH ₄	0.954 (0.725–1.255)	0.737	0.895 (0.643–1.245)	0.510
Type 2 diabetes	H ₂	1.218 (0.566–2.624)	0.798	0.379 (0.031–4.662)	0.448
	CH ₄	0.558 (0.250–1.244)	0.154	0.818 (0.303–2.211)	0.692
	H ₂ /CH ₄	0.843 (0.698–1.194)	0.695	0.769 (0.220–2.695)	0.682
Hypertension	H ₂	1.410 (0.179–11.133)	0.901	0.898 (0.139–5.803)	0.910
	CH ₄	0.853 (0.474–1.536)	0.597	0.941 (0.450–1.965)	0.871
	H ₂ /CH ₄	0.702 (0.344–1.435)	0.333	0.642 (0.261–1.576)	0.333
Smoking	H ₂	0.323 (0.080–1.298)	0.111	0.103 (0.016–0.668)	0.017
	CH ₄	1.185 (0.568–2.470)	0.651	1.335 (0.443–4.027)	0.608
	H ₂ /CH ₄	1.221 (0.489–3.045)	0.669	0.797 (0.211–3.016)	0.738
Alcohol consumption	H ₂	2.286 (0.270–19.381)	0.448	2.765 (0.241–20.533)	0.394
	CH ₄	1.091 (0.547–2.176)	0.804	0.549 (0.179–1.681)	0.294
	H ₂ /CH ₄	1.439 (0.587–3.526)	0.426	1.393 (0.319–6.079)	0.659

Table 2. Univariate and Multivariate logistic regression analyses of factors associated with different type of SIBO. Bold indicates statistically significant difference.

		Total	H ₂ -SIBO	CH ₄ -SIBO	H ₂ /CH ₄ -SIBO	p-value
H ₂	H ₂ 90min AUC	967.5(465,1901.25)	660(442.5,1530)	945(510,1935)	1125(465,2160)	0.322
	H ₂ 90-150min AUC	1020(465,2370)	915(442.5,1822.5)	1125(532.5,2467.5)	1230(525,2955)	0.456
	H ₂ peak	33(14,66)	24(8.25,48.5)	31(14,63)	40(15,73)	0.179
	H ₂ mean	16.8(7.3,32)	15.05(6.08,27.35)	15(7.5,31.3)	19.25(8.3,35.08)	0.277
	H ₂ total AUC	2265(1035,4545)	1830(915,4035)	2235(1065,4642.5)	2775(1245,5055)	0.300
CH ₄	CH ₄ baseline	9(6,14)	5(3,6.5)	10(8,14)	11(7,16.25)	0.001
	CH ₄ final line	11(7,16)	8(4,10)	12(8.25,17)	13(9,19)	0.001
	CH ₄ peak	14(10,20)	8.5(5.25,9.75)	15(11,20)	16(11,24)	<0.001
	CH ₄ mean	11.2(8.5,15.2)	6.5(4.22,8.45)	11(8.8,15.2)	12.6(9.15,17)	<0.001
	CH ₄ total AUC	1582.5(1080,2190)	990(667.5,1267.5)	1650(1312.5,2265)	1860(1335,2505)	0.001
	(CH ₄ + H ₂) total AUC	4080(2370,6630)	3000(2103.75,5223.75)	4725(2820,7125)	4065(2505,6435)	0.031

Table 3. The difference in breath volume and AUC between different subgroups of SIBO. AUC area under the curve. Bold indicates statistically significant difference.

methane and age ($p=0.0249$, $R^2=0.0172$), while no significant association was observed with BMI ($p=0.2654$, $R^2=0.0056$). Overall, these results suggest that age, but not BMI, is positively associated with combined hydrogen and methane expiratory volumes.

Ecological niche partitioning of intestinal microbial communities

Basic characteristics of gut microbiota in the population

At the family level (Fig. 2a,d), *Prevotellaceae* were relatively enriched in the Normal group and reduced in both H₂-SIBO and CH₄-SIBO. In contrast, *Bacteroidaceae*, *Veillonellaceae*, *Ruminococcaceae*, and *Lachnospiraceae* were more abundant in the SIBO groups, with a stronger shift in H₂-SIBO. At the genus level (Fig. 2b,e), *Prevotella*, *Faecalibacterium*, *Roseburia*, *Sutterella*, and *Parabacteroides* were relatively depleted in SIBO, whereas *Bacteroides*, *Blautia*, *Ruminococcus*, and *Clostridium XIVa* were relatively increased.

Characterization of the intestinal microbiota based on α - and β -diversity

We analyzed gut microbiota alpha diversity to compare SIBO patients with healthy controls. Measures including the Chao1, Shannon, Simpson indices, and observed species counts showed no significant differences among the Normal, H₂-SIBO, and CH₄-SIBO groups (Fig. 2g–j), indicating comparable microbial richness and evenness across groups. Pairwise PERMANOVA analyses revealed a significant separation in β -diversity between the Normal and H₂-SIBO groups ($R=0.099$, $p=0.008$). In contrast, differences between Normal and CH₄-SIBO ($R=0.065$, $p=0.174$), as well as between H₂-SIBO and CH₄-SIBO ($R=0.068$, $p=0.171$), were not statistically significant (Fig. 3a,b), suggesting that alterations in community structure were more pronounced in H₂-SIBO than in CH₄-SIBO.

LEfSe analysis of microbial biomarkers

We applied LEfSe analysis to compare microbiome differences among the Normal, CH₄-SIBO, and H₂-SIBO groups (Fig. 3c,d). Distinct microbial signatures characterized each group, as indicated by significant LDA scores. The Normal group was primarily characterized by an enrichment of taxa including *Bacilli*, *Lactobacillales*, and *Enterobacter cloacae*. These taxa are commonly associated with the maintenance of gut homeostasis, with *Lactobacillales* being recognized as important probiotics. The CH₄-SIBO group showed a significant enrichment of *Bacteroidaceae* and *Bacteroides*. This specific signature suggests that these taxa may be implicated in the microbial dysbiosis and metabolic processes associated with methane overproduction. In contrast, the H₂-SIBO subtype showed a broader and more diverse pattern of enrichment across multiple taxonomic ranks. Significant increases were observed at the class and order levels (*Betaproteobacteria* and *Burkholderiales*), at the family level (*Alcaligenaceae* and *Acidaminococcaceae*), and at the genus level (*Bacteroides*, *Sutterella*, *Phascolarctobacterium*, and an unclassified genus).

Basic characteristics of gut microbiota metabolites

Fecal metabolomic profiling of the Normal, CH₄-SIBO, and H₂-SIBO groups was examined using PCA, PCoA, and OPLS-DA (Fig. 4a–c). The unsupervised PCA and PCoA plots showed partial overlap among groups, suggesting broadly similar overall metabolomic structure. By contrast, the supervised OPLS-DA model suggested group separation; however, this observation should be interpreted cautiously because the sample size was small and supervised models are prone to overfitting.

Volcano-plot analysis identified 85 differential metabolites between CH₄-SIBO and H₂-SIBO, 40 between H₂-SIBO and the Normal group, and 52 between CH₄-SIBO and the Normal group according to the prespecified screening criteria (Fig. 4d–f). Highlighted metabolites included palmitic acid and tryptophyl-proline, which were relatively increased in the positive groups, whereas demethoxycurcumin and 5-chloro-4(3H)-quinazolinone were relatively enriched in the Normal group (Fig. 4g).

KEGG pathway enrichment implicated valine, leucine, and isoleucine biosynthesis together with mineral absorption pathways, suggesting altered amino acid-related and nutrient-related metabolism across subtypes

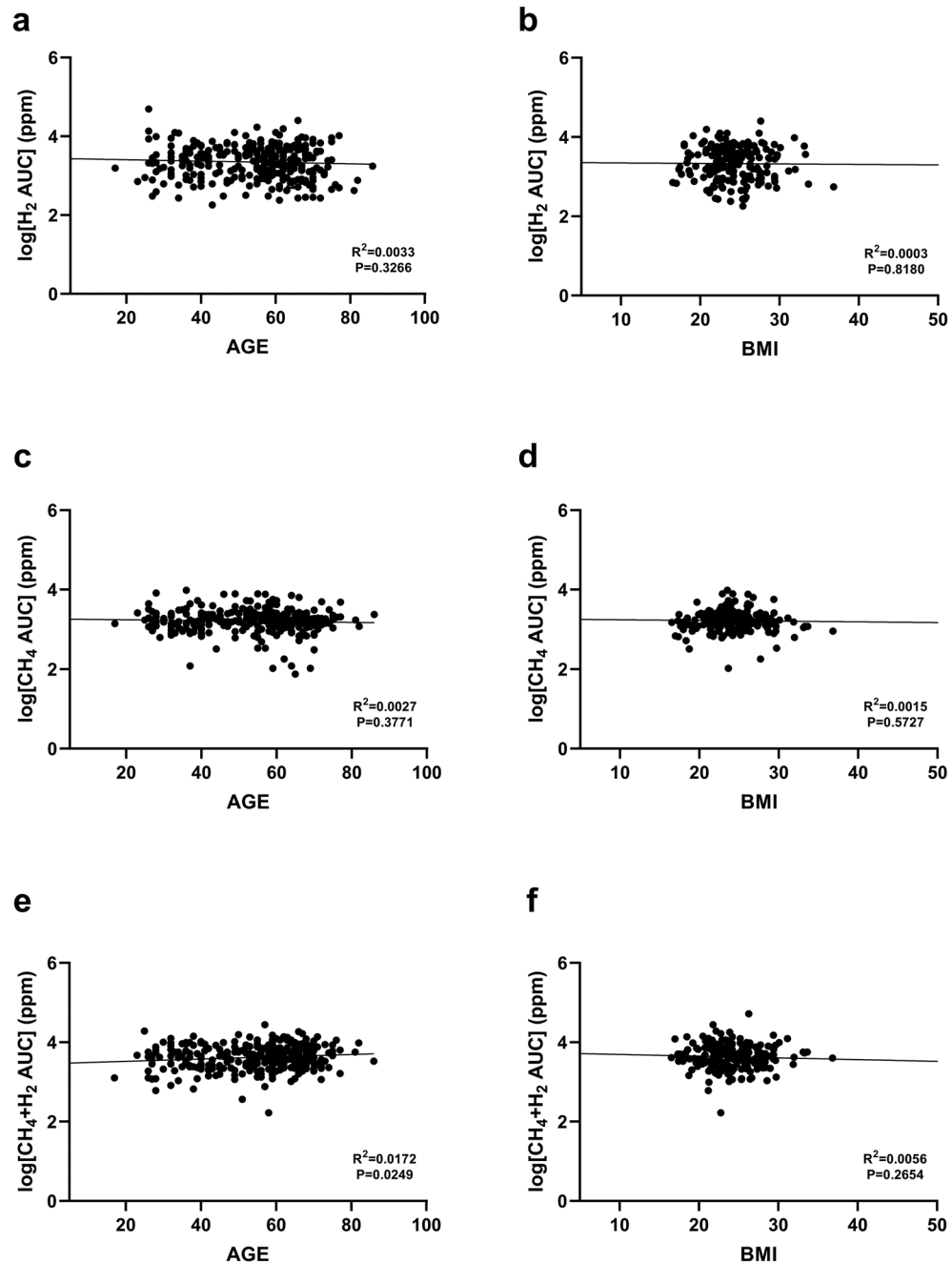


Fig. 1. Linear correlations between expiratory hydrogen and methane volumes and patient characteristics. (a,b) Correlation of hydrogen (H_2) area under the curve (AUC) with age and BMI. (c,d) Correlation of methane (CH_4) AUC with age and BMI. (e,f) Correlation of combined hydrogen and methane ($H_2 + CH_4$) AUC with age and BMI.

(Fig. 5a). Because these analyses were exploratory and based on nominal screening thresholds, pathway findings should be interpreted as hypothesis-generating.

Correlation analysis between gut microbiota and metabolites

To further explore the relationships between gut microbiota and microbial metabolism in CH_4 -SIBO and H_2 -SIBO patients, Spearman correlation analysis was performed (Fig. 5b,c). Tyr-Val showed a significant negative correlation with Actinomycetaceae, while 5-O-Methylnaringenin was positively correlated with Alcaligenaceae. Additionally, metabolites such as palmitic acid and 3,4-diaminoisole displayed significant positive or negative correlations with multiple bacterial families, indicating their potential roles in modulating gut microbial metabolic functions.

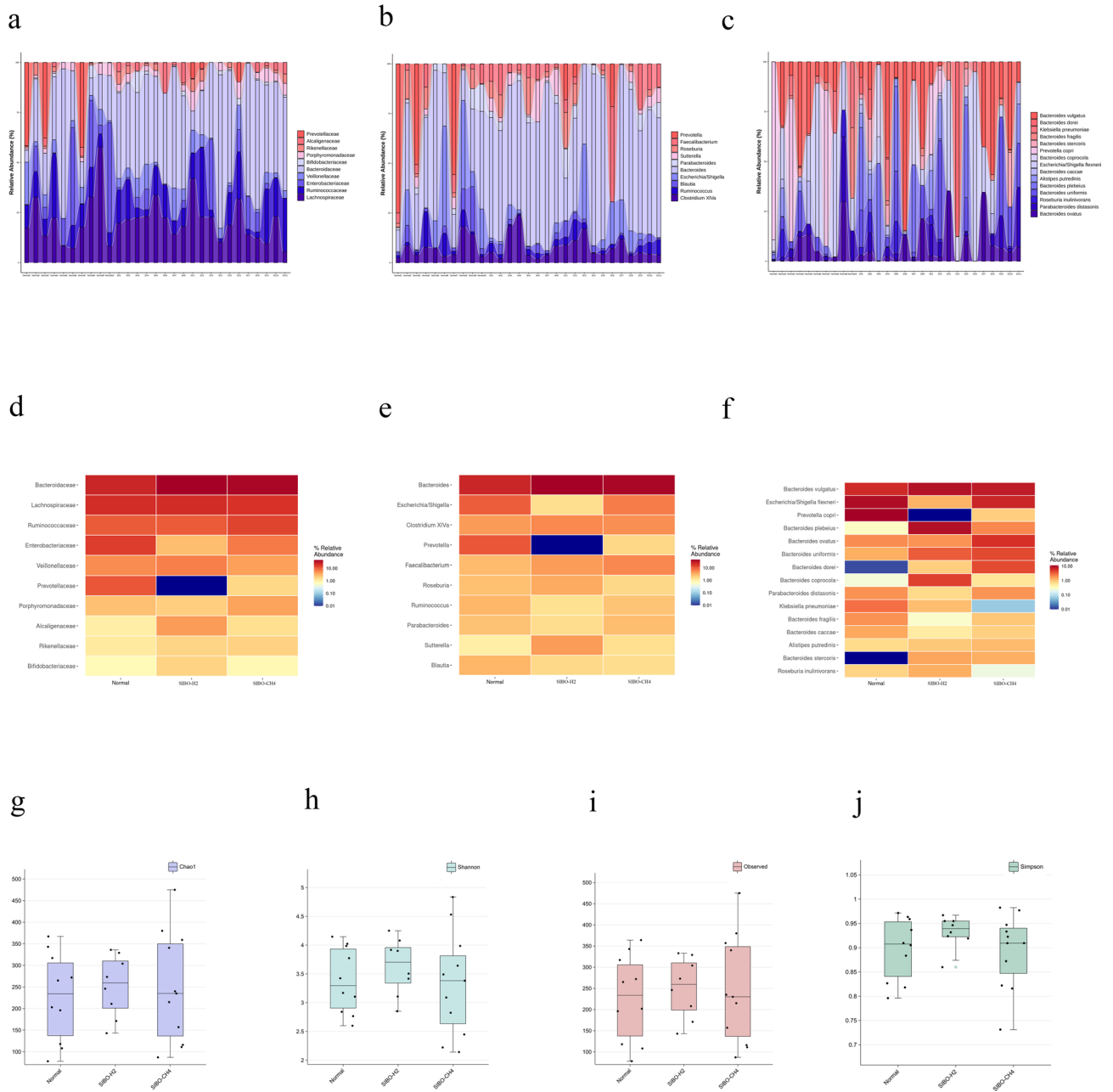


Fig. 2. Stacked bar plots showing the taxonomic composition of individual samples at the family level (a), top 10 genera by abundance (b), and top 15 species by abundance (c). (d) Distribution of intestinal microbiome at the family level for each of the three groups, (e) top 10 genera by abundance, and (f) top 15 species by abundance. (g) Alpha diversity based on the Chao1 index between groups; (h) alpha diversity based on the Shannon index between groups; (i) alpha diversity based on the Observed index between groups; (j) alpha diversity based on the Simpson index between groups.

Discussion

Key clinical and pathophysiological insights into SIBO and subtypes

In this study, we systematically analyzed clinical and laboratory data from SIBO-positive patients and investigated factors associated with H₂- and CH₄-SIBO. In interpreting the high prevalence of SIBO observed in our cohort, it is important to consider regional dietary patterns as a potential contributing factor. Northern Chinese populations—where our hospital is located—consume diets heavily enriched in carbohydrates, with wheat-based staples such as noodles and steamed buns predominating. Although participants adhered to pre-test fasting and dietary restrictions designed to minimize acute fermentation effects prior to breath testing, habitual long-term dietary patterns cannot be modified in the short term. Chronic exposure to high-carbohydrate diets may predispose individuals to enhanced intestinal fermentation, thereby increasing baseline breath hydrogen and methane production and the likelihood of positive SIBO tests^{21,22}. These regional dietary influences may

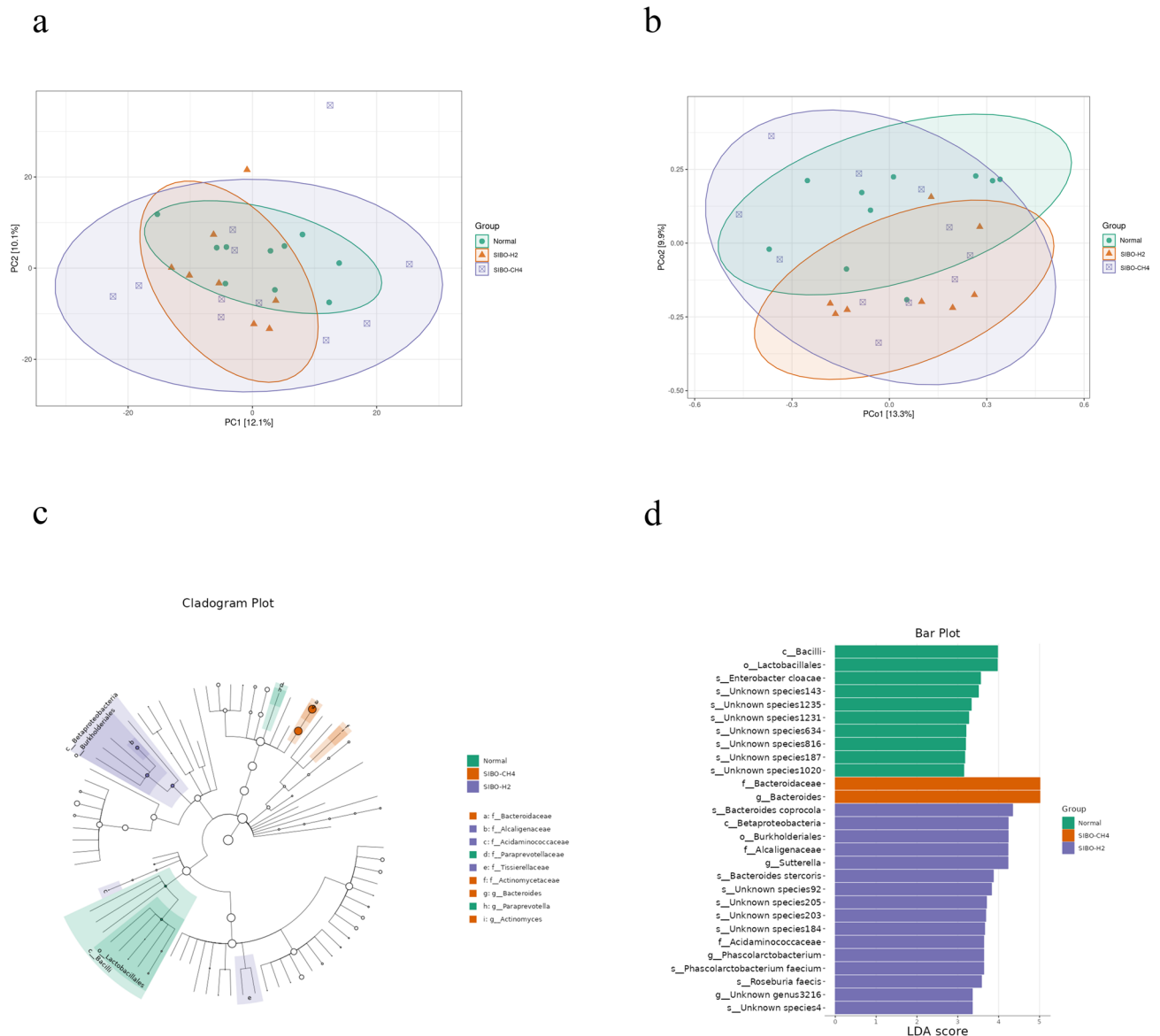


Fig. 3 applied LefSe analysis to compare microbiome differences among the . Gut microbiota community structure and differential taxa analysis. **(a)** Principal component analysis (PCA). **(b)** Principal coordinates analysis (PCoA). **(c,d)** LefSe analysis identifying phylogenetic differences between groups. Only taxa with linear discriminant analysis (LDA) scores > 2 are shown.

also partly explain the observed associations between branched-chain amino acid levels and SIBO subtypes. As such, while our findings suggest potential mechanistic links between microbial activity and host metabolism, they should be interpreted in the context of local dietary habits. Future studies incorporating multi-regional cohorts or controlling for long-term dietary intake will be necessary to validate the generalizability of these associations.

Our results demonstrate that serum glucose levels are independent predictors of CH₄-predominant SIBO, whereas albumin and smoking are significantly associated with H₂-SIBO. These findings highlight distinct host and metabolic factors underlying gas-specific SIBO phenotypes. For H₂-SIBO, serum albumin was the biochemical variable that remained independently associated with increased odds of H₂-SIBO in both univariable and multivariable analysis; no variable reached statistical significance in multivariable

analysis. Higher albumin levels may reflect preserved hepatic synthetic function or altered protein-energy metabolism that favors hydrogenogenic bacterial activity; however, the underlying mechanisms require further investigation⁴⁷. Smoking showed a significant inverse association with H₂-SIBO after adjustment, despite a nonsignificant trend in univariable analysis. Prior studies indicate that tobacco exposure can modify gastrointestinal motility, mucosal immunity, and microbial composition^{23–26}, which may partially account for the reduced likelihood of hydrogen-producing bacterial overgrowth in certain physiological contexts. Elevated total bilirubin can weaken bile acid-mediated antimicrobial activity and antioxidant defense, increasing mucosal

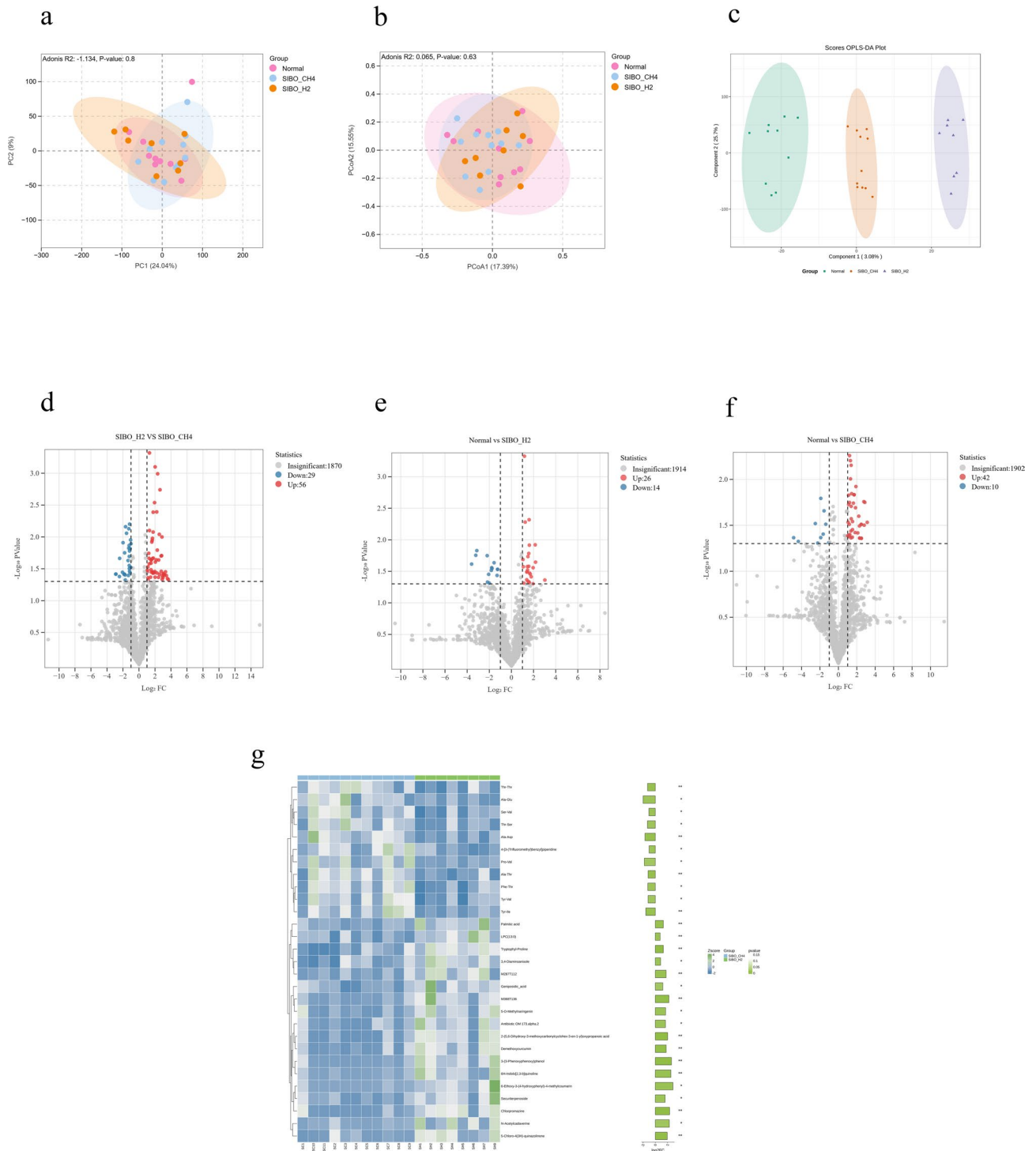


Fig. 4. Metabolomic analysis of gut microbiota metabolites in each group (* : $p < 0.05$; ** : $p < 0.01$). (a) PCA based on intestinal microbiome metabolites; (b) PCoA plot based on intestinal microbiome metabolites; (c) OPLS-DA analysis based on intestinal microbiome metabolites. Volcano plots of differential metabolites among the three groups: (d) H₂-SIBO vs. CH₄-SIBO; (e) healthy control group vs. H₂-SIBO; (f) healthy control group vs. CH₄-SIBO. (g) Heatmap of differential metabolites.

susceptibility^{27–29}. Lower alkaline phosphatase activity may impair detoxification of bacterial endotoxins, promoting mucosal inflammation, while higher triglycerides levels reflect lipid metabolic disturbances that support anaerobic growth and delayed intestinal transit^{30–32}. These factors may collectively shape a luminal environment more favorable for hydrogen-producing bacteria, although their contributions appear secondary to albumin and smoking based on the adjusted regression results.

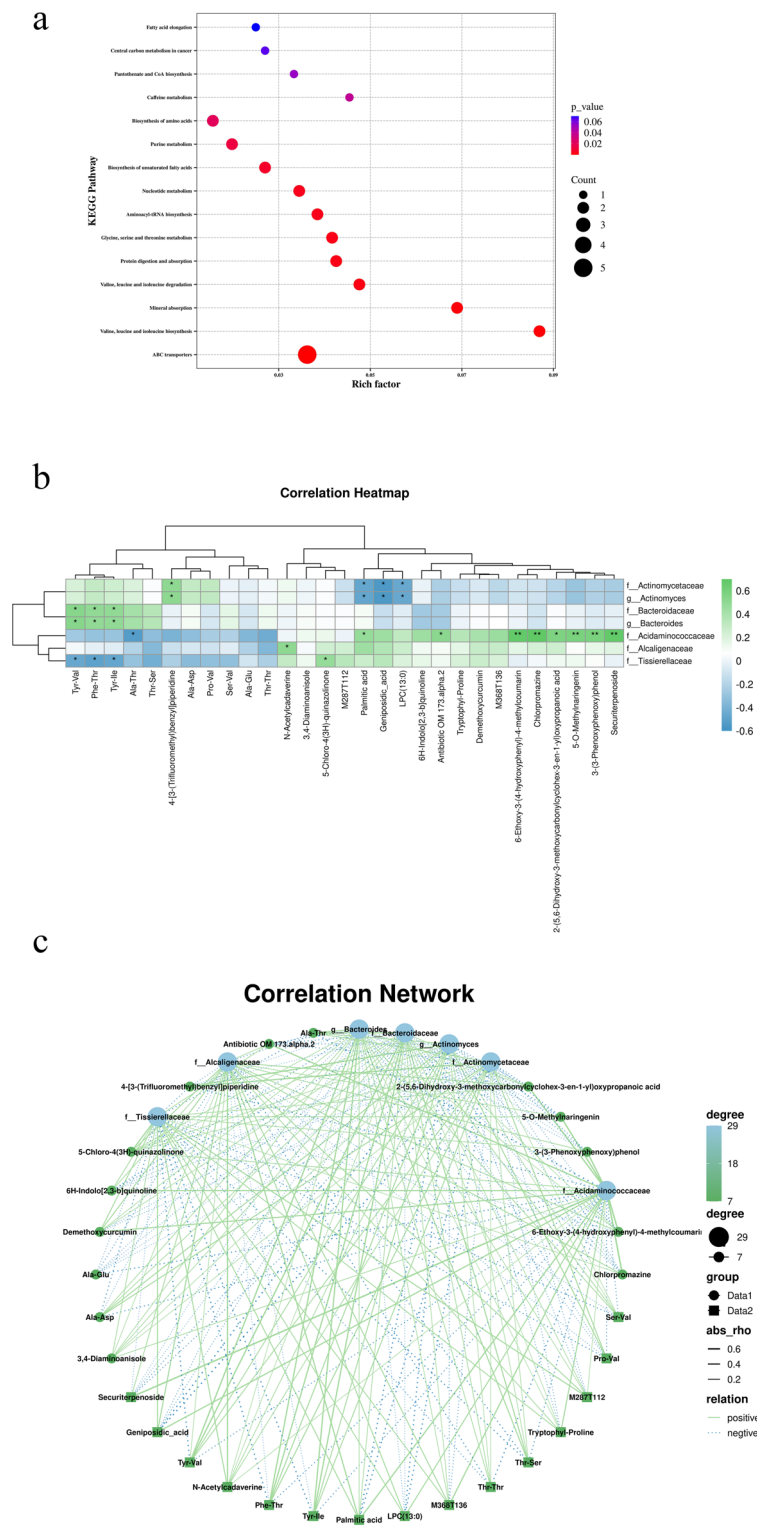


Fig. 5. (a) KEGG pathway enrichment of differential metabolites. (b) Spearman correlation heatmap between selected microbial taxa and metabolites, where green indicates positive correlation and blue indicates negative correlation (* p < 0.05; ** p < 0.01). (c) Correlation network linking selected microbial taxa and metabolites; solid green lines indicate positive correlations and dashed blue lines indicate negative correlations.

For CH₄-SIBO, higher glucose levels were the factor that maintained statistical significance in both analytic stages. *Methanogenic archaea* rely on fermentation-derived substrates such as hydrogen, formate, and carbon dioxide; thus, elevated systemic glucose may reflect metabolic states that promote substrate availability and niche expansion for methane producers. Although prior work links impaired glucose metabolism with altered transit

and fermentation capacity^{33,34}, further mechanistic studies are warranted. Other host variables—including albumin, diabetes status, smoking, hypertension, and alcohol intake—were not independently associated with CH₄-SIBO in the adjusted model, suggesting that methane overgrowth may be driven by a more restricted set of metabolic determinants.

For the mixed H₂/CH₄ subtype, no variable reached statistical significance in multivariable analyses. This absence of clear associations may indicate that mixed-gas patterns represent heterogeneous microbial configurations or transitional states in which host metabolic factors exert weaker or more diffuse influences. Such variability has been documented in studies demonstrating instability of mixed fermentation phenotypes over time^{27–29}.

Distinct role of methane expiratory volume in SIBO subgroup differentiation

We analyzed the correlation between expiratory methane volume and SIBO subgroups by examining total, average, and peak gas volumes. Methane expiratory volume was significantly associated with SIBO subgroups, whereas hydrogen expiratory volume was not. This distinction reflects the differential metabolic roles of the gut microbiota in each subgroup. In the CH₄-SIBO group, dominated by methanogens such as *Methanobrevibacter smithii*, methane production relies on hydrogen utilization but is also modulated by the intestinal environment. Consequently, methane volume serves as a reliable marker of methanogen activity and proliferation, supporting its use as a key diagnostic indicator for CH₄-SIBO. In contrast, hydrogen levels are consumed by methanogens and utilized by diverse gut microbes, which may explain the lack of correlation with subgroup identification and limits its specificity. Methane itself can slow intestinal transit, creating a feedback loop that further promotes methanogen overgrowth and hydrogen consumption. Therefore, expiratory methane volume not only reflects microbial activity but may also contribute to altered gut motility, highlighting the mechanistic role of methane in SIBO pathogenesis. These findings reinforce the clinical utility of hydrogen-methane breath tests in differentiating SIBO phenotypes.

Previous studies have suggested that age and BMI may influence expiratory gas volumes³⁵. In our cohort, age positively correlated with total gas volumes, potentially reflecting age-related alterations in gut microbiota composition, slower intestinal transit, dietary changes, and declining immune function, all of which can facilitate gas production and bacterial overgrowth^{36–38}. In contrast, no significant association was observed between BMI and gas volumes, consistent with prior research³⁹. This may be due to BMI being a relatively crude proxy for gut microbial composition, with dietary habits and metabolic factors potentially influencing gas production indirectly.

Distinct gut microbiota profiles and metabolic characteristics in SIBO subtypes

To investigate gut microbiota differences between SIBO subtypes, we performed 16S rRNA sequencing on stool samples from H₂-SIBO and CH₄-SIBO patients. Significant variations in bacterial family abundances were observed. Both groups showed increased *Bacteroidaceae*, *Veillonellaceae*, *Ruminococcaceae*, and *Lachnospiraceae*, with a stronger increase in the H₂-SIBO group. Conversely, *Rikenellaceae*, *Porphyromonadaceae*, and *Bifidobacteriaceae* decreased in both groups⁷. In the CH₄-SIBO group, *Bacteroidaceae*, particularly *Bacteroides* and *Bacteroides coprocola*, were enriched. These bacteria metabolize complex carbohydrates and generate fermentation end products, including hydrogen and short-chain fatty acids, which may serve as substrates for methanogenic archaea, thereby indirectly promoting methane overproduction. This overgrowth impairs intestinal motility and worsens symptoms like bloating and constipation^{40,41}. Additionally, their activity may disrupt gut redox balance, nutrient absorption, and immune responses, creating a vicious cycle. The H₂-SIBO group was characterized by higher levels of *Alcaligenaceae* and *Sutterella*. These taxa have been associated with altered gut fermentation and gas production. *Sutterella*'s complex metabolic interactions can affect gut motility and immune function, potentially impairing the intestinal barrier and exacerbating dysbiosis^{42,43}. Overall, the H₂-SIBO and CH₄-SIBO subtypes show distinct microbial profiles and metabolic impacts on gut function. Recognizing these differences is critical for identifying specific biomarkers and developing targeted treatments tailored to each subtype, ultimately improving clinical outcomes in SIBO patients.

Our analysis of gut microbiota metabolites across SIBO subgroups highlights the valine, leucine, and isoleucine (Branched-Chain Amino Acid Metabolism Pathway, BCAA) biosynthetic pathway as a key perturbed metabolic route, as revealed by KEGG enrichment analysis. This hypothesizes substantial alterations in BCAA metabolism associated with SIBO. Overgrowth of anaerobic and metabolically active bacteria may enhance BCAA pathway activity, potentially through increased degradation of dietary proteins and host-derived amino acids, thereby reshaping the gut metabolic environment⁴⁴. Enhanced BCAA metabolism potentially supports the survival and growth of specific microbial taxa. For example, hydrogen-producing bacteria in the H₂-SIBO subgroup require high energy availability, which may be facilitated by BCAA-derived metabolites⁴⁵. Similarly, methanogens in the CH₄-SIBO subgroup could indirectly benefit from BCAA metabolites via microbial interactions. Importantly, altered BCAA metabolism may also impact host physiology. Elevated BCAA levels have been associated with impaired intestinal barrier function, increased oxidative stress, and exacerbation of intestinal inflammation, which may contribute to dysbiosis⁴⁶. Accumulation of BCAA metabolites in SIBO patients could further influence systemic metabolism via the hepatoenteric axis, potentially linking microbial metabolic changes to metabolic syndrome and insulin resistance⁴⁷.

Given the moderate sample size of this study, these findings should be interpreted as preliminary observations, suggesting potential mechanistic links rather than definitive causal relationships. Nonetheless, the observed alterations in the BCAA biosynthetic pathway provide insights into subtype-specific microbial metabolism in SIBO and may inform future strategies targeting metabolic modulation for personalized interventions.

Limitations

This study has several limitations. First, the relatively small sample size may have reduced statistical power, particularly for identifying modest associations across different SIBO subtypes. Second, the single-center design may limit the generalizability of the findings, as the study population may not fully represent broader geographic or ethnic variability. Third, although 16S rRNA sequencing combined with the ASV approach using DADA2 provides higher-resolution insights into microbial community structure compared with traditional OTU clustering, it still has limited capacity to fully resolve strain-level differences or capture functional potential. Complementary metagenomic or metatranscriptomic analyses would be required to comprehensively characterize functional and strain-level microbial dynamics. Finally, the cross-sectional design precludes causal inference; therefore, observed associations between microbiota alterations, clinical variables, and SIBO subtypes should be interpreted as correlational. Longitudinal studies and mechanistic experiments are needed to clarify underlying causal pathways.

Conclusion

In this study, breath-test-positive participants were classified into three SIBO phenotypes based on hydrogen and methane profiles. Significant clinical differences were observed across subtypes, with higher albumin levels in H₂-SIBO and higher fasting glucose levels in CH₄-SIBO. Methane-related expiratory measures, but not hydrogen-related measures, differed significantly across subtypes, and age was positively associated with combined expiratory gas volume. Distinct stool microbial patterns were also observed: H₂-SIBO was enriched in *Alcaligenaceae* and *Sutterella*, whereas CH₄-SIBO showed higher abundance of *Bacteroidaceae*, *Bacteroides*, and *Bacteroides coprocola*. Metabolomic analysis suggested alterations in BCAA-related pathways. Overall, these findings support the presence of potential subtype-specific microbial and metabolic signatures in SIBO, while also underscoring the need for larger prospective studies to clarify causality and clinical utility.

Data availability

Some clinical data are not publicly available because of privacy considerations. De-identified data may be obtained from the corresponding author on reasonable request. The gut microbiome datasets generated in this study have been deposited in the NCBI Sequence Read Archive under accession number PRJNA1269711.

Received: 25 October 2025; Accepted: 9 March 2026

Published online: 19 March 2026

References

- Martino, C. et al. Microbiota succession throughout life from the cradle to the grave. *Nat. Rev. Microbiol.* **20** (12), 707–720 (2022).
- Aljadah, M. & Widlansky, M. E. Finding needles in the gut microbiota's haystack. *Circ. Res.* **132** (2), 182–184 (2023).
- Geva-Zatorsky, N. et al. Mining the human gut microbiota for immunomodulatory organisms. *Cell* **168** (5), 928–943.e11 (2017).
- Revaiah, P. C. et al. Risk of small intestinal bacterial overgrowth in patients receiving proton pump inhibitors versus proton pump inhibitors plus prokinetics. *JGH Open Access J. Gastroenterol. Hepatol.* **2** (2), 47–53 (2018).
- Zmora, N., Suez, J. & Elinav, E. You are what you eat: Diet, health and the gut microbiota. *Nat. Rev. Gastroenterol. Hepatol.* **16** (1), 35–56 (2019).
- Manson, J. M., Rauch, M. & Gilmore, M. S. The commensal microbiology of the gastrointestinal tract. *Adv. Exp. Med. Biol.* **635**, 15–28 (2008).
- Banaszak, M., Górna, I., Woźniak, D., Przysławski, J. & Drzymala-Czyż, S. Association between gut dysbiosis and the occurrence of SIBO, LIBO, SIFO and IMO. *Microorganisms* **11** (3), 573 (2023).
- Skrzydło-Radomska, B. & Cukrowska, B. How to recognize and treat small intestinal bacterial overgrowth?. *J. Clin. Med.* **11** (20), 6017 (2022).
- Vernia, P., Cesarini, M., de Carolis, A. & Vernia, F. Early hydrogen excretion peaks during breath tests. Small intestinal bacterial overgrowth or accelerated transit?. *Dig. Liver Dis.* **53** (4), 442–444 (2021).
- Yokoyama, K. et al. Hydrogen-producing small intestinal bacterial overgrowth is associated with hepatic encephalopathy and liver function. *PLoS ONE* **17** (2), e0264459 (2022).
- Madigan, K. E., Bundy, R. & Weinberg, R. B. Distinctive clinical correlates of small intestinal bacterial overgrowth with methanogens. *Clin. Gastroenterol. Hepatol. Off. Clin. Pract. J. Am. Gastroenterol. Assoc.* **20** (7), 1598–1605.e2 (2022).
- Mello, C. S. et al. Methane production and small intestinal bacterial overgrowth in children living in a slum. *World J. Gastroenterol.* **18** (41), 5932–5939 (2012).
- Jung, S. E., Joo, N. S., Han, K. S. & Kim, K. N. Obesity is inversely related to hydrogen-producing small intestinal bacterial overgrowth in non-constipation irritable bowel syndrome. *J. Korean Med. Sci.* **32** (6), 948–953 (2017).
- Houben, E., De Preter, V., Billen, J., Van Ranst, M. & Verbeke, K. Additional value of CH₄ measurement in a combined ¹³C/H₂ lactose malabsorption breath test: A retrospective analysis. *Nutrients* **7** (9), 7469–7485 (2015).
- Quigley, E. M. M., Murray, J. A. & Pimentel, M. AGA clinical practice update on small intestinal bacterial overgrowth: Expert review. *Gastroenterology* **159** (4), 1526–1532. <https://doi.org/10.1053/j.gastro.2020.06.090> (2020).
- Nejman, D. et al. The human tumor microbiome is composed of tumor type-specific intracellular bacteria. *Science* **368** (6494), 973–980 (2020).
- Mishra, A. et al. Microbial exposure during early human development primes fetal immune cells. *Cell* **184** (13), 3394–3409.e20 (2021).
- Parhi, L. et al. Breast cancer colonization by *Fusobacterium nucleatum* accelerates tumor growth and metastatic progression. *Nat. Commun.* **11** (1), 3259 (2020).
- Kanehisa, M., Furumichi, M., Sato, Y., Matsuura, Y. & Ishiguro-Watanabe, M. KEGG: Biological systems database as a model of the real world. *Nucleic Acids Res.* **53** (D1), D672–D677. <https://doi.org/10.1093/nar/gkae909> (2025).
- Kanehisa, M. & Goto, S. KEGG: Kyoto encyclopedia of genes and genomes. *Nucleic Acids Res.* **28** (1), 27–30. <https://doi.org/10.1093/nar/28.1.27> (2000).
- Riordan, S. M., McIver, C. J. & Williams, R. Liver damage in human small intestinal bacterial overgrowth. *Am. J. Gastroenterol.* **93** (2), 234–237 (1998).
- Zhang, Y., Feng, Y., Cao, B. & Tian, Q. The effect of small intestinal bacterial overgrowth on minimal hepatic encephalopathy in patients with cirrhosis. *Arch. Med. Sci. AMS* **12** (3), 592–596 (2016).

23. Wang, L. et al. The bidirectional gut-lung axis in chronic obstructive pulmonary disease. *Am. J. Respir. Crit. Care Med.* **207** (9), 1145–1160 (2023).
24. Fan, J. et al. Cross-talks between gut microbiota and tobacco smoking: a two-sample Mendelian randomization study. *BMC Med.* **21** (1), 163 (2023).
25. Bai, X. et al. Cigarette smoke promotes colorectal cancer through modulation of gut microbiota and related metabolites. *Gut* **71** (12), 2439–2450 (2022).
26. Lai, H.-C. et al. Gut microbiota modulates COPD pathogenesis: role of anti-inflammatory Parabacteroides goldsteinii lipopolysaccharide. *Gut* **71** (2), 309–321 (2022).
27. Hasuike, Y. et al. Bile acid abnormality induced by intestinal dysbiosis might explain lipid metabolism in Parkinson's disease. *Med. Hypotheses* **134**, 109436 (2020).
28. Vitek, L., Zelenka, J., Zadinová, M. & Malina, J. The impact of intestinal microflora on serum bilirubin levels. *J. Hepatol.* **42** (2), 238–243 (2005).
29. Tuzun, F., Kumral, A., Duman, N. & Ozkan, H. Breast milk jaundice: Effect of bacteria present in breast milk and infant feces. *J. Pediatr. Gastroenterol. Nutr.* **56** (3), 328–332 (2013).
30. Jiang, H. et al. The fecal microbiota of patients with primary biliary cholangitis (PBC) causes PBC-like liver lesions in mice and exacerbates liver damage in a mouse model of PBC. *Gut Microb.* **16** (1), 2383353 (2024).
31. Liu, Y. et al. Risk factors for small intestinal bacterial overgrowth in patients with acute ischaemic stroke. *J. Med. Microbiol.* <https://doi.org/10.1099/jmm.0.001666> (2023).
32. Kvit, K. B. et al. The role of small intestinal bacterial overgrowth in the pathogenesis of hyperlipidemia. *Wiad. Lek.* **72** (4), 645–649 (2019).
33. Ma, Q. et al. Research progress in the relationship between type 2 diabetes mellitus and intestinal flora. *Biomed. Pharmacother.* **117**, 109138 (2019).
34. Guo, X. et al. Interactive relationships between intestinal flora and bile acids. *Int. J. Mol. Sci.* **23** (15), 8343 (2022).
35. Aron-Wisniewsky, J., Warmbrunn, M. V., Nieuwdorp, M. & Clément, K. Metabolism and metabolic disorders and the microbiome: The intestinal microbiota associated with obesity, lipid metabolism, and metabolic health-pathophysiology and therapeutic strategies. *Gastroenterology* **160** (2), 573–599 (2021).
36. Almeida, J. A. et al. Lactose malabsorption in the elderly: Role of small intestinal bacterial overgrowth. *Scand. J. Gastroenterol.* **43** (2), 146–154 (2008).
37. Ling, Z., Liu, X., Cheng, Y., Yan, X. & Wu, S. Gut microbiota and aging. *Crit. Rev. Food Sci. Nutr.* **62** (13), 3509–3534 (2022).
38. Du, Y. et al. Effects of anti-aging interventions on intestinal microbiota. *Gut Microbes* **13** (1), 1994835 (2021).
39. Allegretti, J. R. et al. Effects of fecal microbiota transplantation with oral capsules in obese patients. *Clin. Gastroenterol. Hepatol.* **18** (4), 855–863.e2 (2020).
40. Wexler, H. M. Bacteroides: The good, the bad, and the nitty-gritty. *Clin. Microbiol. Rev.* **20** (4), 593–621 (2007).
41. Vallianou, N. G. et al. The role of next-generation probiotics in obesity and obesity-associated disorders: Current knowledge and future perspectives. *Int. J. Mol. Sci.* **24** (7), 6755 (2023).
42. Kaakoush, N. O. Sutterella species, IgA-degrading bacteria in ulcerative colitis. *Trends Microbiol.* **28** (7), 519–522 (2020).
43. Pinart, M. et al. Gut microbiome composition in obese and non-obese persons: A systematic review and meta-analysis. *Nutrients* **14** (1), 12 (2021).
44. Lynch, C. J. & Adams, S. H. Branched-chain amino acids in metabolic signalling and insulin resistance. *Nat. Rev. Endocrinol.* **10** (12), 723–736 (2014).
45. De Santis, M. C., Bockorny, B., Hirsch, E., Cappello, P. & Martini, M. Exploiting pancreatic cancer metabolism: Challenges and opportunities. *Trends Mol. Med.* **30** (6), 592–604 (2024).
46. Dimou, A., Tsimihodimos, V. & Bairaktari, E. The critical role of the branched chain amino acids (BCAAs) catabolism-regulating enzymes, branched-chain aminotransferase (BCAT) and branched-chain α -keto acid dehydrogenase (BCKD), in human pathophysiology. *Int. J. Mol. Sci.* **23** (7), 4022 (2022).
47. Pedersen, H. K. et al. Human gut microbes impact host serum metabolome and insulin sensitivity. *Nature* **535** (7612), 376–381 (2016).

Author contributions

Ziteng Wang, Wentao Tan, Pengfei Zhang, Huanhuan Xiong, Licun Zhu and Jiali Huang were responsible for data acquisition and experiment execution. Lingling He and Ziteng Wang performed data analysis and interpretation. Ziteng Wang and Wentao Tan drafted the manuscript. Hongshan Wei and Hong Liu critically revised the manuscript and supervised the overall work. All authors reviewed and approved the final version of the manuscript and agreed to be accountable for all aspects of the work.

Declarations

Competing interests

The authors declare no competing interests.

Ethics approval and informed consent

This study was conducted in accordance with the Declaration of Helsinki and was approved by the Ethics Committee of Beijing Shijitan Hospital, Capital Medical University (approval no. sjtky11-1x-2022[063]).

Informed consent

Written informed consent was obtained from participants who provided stool samples for microbiome and metabolomic analyses. Handling of retrospective clinical data was performed in accordance with the approved ethics protocol.

Additional information

Correspondence and requests for materials should be addressed to H.W. or H.L.

Reprints and permissions information is available at www.nature.com/reprints.

Publisher's note Springer Nature remains neutral with regard to jurisdictional claims in published maps and institutional affiliations.

Open Access This article is licensed under a Creative Commons Attribution-NonCommercial-NoDerivatives 4.0 International License, which permits any non-commercial use, sharing, distribution and reproduction in any medium or format, as long as you give appropriate credit to the original author(s) and the source, provide a link to the Creative Commons licence, and indicate if you modified the licensed material. You do not have permission under this licence to share adapted material derived from this article or parts of it. The images or other third party material in this article are included in the article's Creative Commons licence, unless indicated otherwise in a credit line to the material. If material is not included in the article's Creative Commons licence and your intended use is not permitted by statutory regulation or exceeds the permitted use, you will need to obtain permission directly from the copyright holder. To view a copy of this licence, visit <http://creativecommons.org/licenses/by-nc-nd/4.0/>.

© The Author(s) 2026